Chapter VI

Phase Transformation and Grain Growth in Spray Deposited Wurtzite $CuInS_2$ Films

VI.1 Introduction

The vacuum processed (mainly co-evaporation and sequential processing techniques) $CuIn_xGa_{1-x}(S,Se)_2$ (CIGS) based solar cells show power conversion efficiencies exceeding 20% [241, 242]. Inherently, vacuum-based processing techniques are expensive and involve high installation and maintenance costs [21, 22, 123, 243, 244]. Therefore, several research groups focus on alternative solution-based deposition approaches that promise high throughput, cost savings, and low energy input [137]. Typically, screen printing [245], doctor blade [53], inkjet printing [246] and spray deposition [28, 247, 248] methods are high-throughput, scalable technologies, where dissolved precursors or pre-synthesized nanoparticles ink is deposited and heat treated to form the final absorber film.

CIS exhibit three different crystal structures: chalcopyrite (tetragonal), zincblende (cubic), and wurtzite (hexagonal) [89]. Chalcopyrite is the thermodynamically stable phase at room temperature with a body-centered tetragonal structure, where sulphur anions are arranged in ABCABC stacking, while the cations (Cu and In) occupy tetrahedral interstitial sites in an ordered fashion. At higher temperatures (around 980 °C), due to the disordering of the cations, each chalcopyrite unit cell

gives rise to two unit cells of zinc blend structure arranged one over another along the *c* direction [89]. On further heating to 1090 °C, the stacking sequence of sulphur planes ((111) of zinc blend) changes to …ABAB… assuming a wurtzite structure with (0002) being the equivalent close-packed plane of anionic sublattice [47, 89]. Chalcopyrite CISSe has been reported to exhibit the highest PCE compared to the other allotropes [15, 243], mainly due to its suitable bandgap (1.1-1.7 eV) [249], absorption coefficient ($>10^5 cm^{-1}$) [250], and the lattice constants nearly matching with the buffer layer CdS [61, 82].

Recently, wurtzite (wz) nanoparticle inks have been successfully utilized to fabricate kesterite (ks) Cu_2ZnSnS_4(CZTS) films [38, 39, 41, 43, 251]. The key to this robust fabrication method has been the reactive sintering accompanied by wurtzite to kesterite phase transformation when exposed to selenium [41,43] or sulfur [38, 39, 251] vapor at high temperature, forming micron-sized grains. It was stated that for sulfurization/selenization of stable phase kesterite CZTS absorber film, the driving force for grain growth is a reduction in total energy allied with the high surface area of NPs [39]. The wz-CZTS NPs being metastable, it adds to the driving force to form the stable ks-CZTS phase during selenization [39, 41]. This makes wz-CZTS NPs much more favorable as starting material instead for the formation of large grained ks-CZTS. Similar to the CZTS, CIS/CIGS also exhibits wurtzite to the thermodynamically stable chalcopyrite phase transformation on heating. However, wurtzite to chalcopyrite phase transformation has not been explored extensively to process the CIS/CIGS absorber films [47, 252].

In this chapter, we have studied the phase transformation and grain growth of wz-CIS during selenization. Solution-processed wz-CIS nanoparticles (NPs) ink was

deposited on soda-lime glass (SLG) and Mo-coated SLG substrates by spray deposition. The films were selenized to convert wz-CIS NPs films into large-grained ch-CISSe. The phase analysis, film microstructure and changes in chemical composition due to selenization was investigated.

VI.2 A Review of Relevant Literature

Large elongated grains are preferred for the application as a PV absorber, which is generally achieved after the selenization [141, 143, 145, 152, 253]. In addition, selenization process reduces the defect density, thereby, improving the carrier transport properties [40]. A compact, adherent, and void-free large-grained morphology is vital for achieving reduced electron-hole recombination rate and high device performance [27, 60, 251]. Generally, solution processing of CIGS films utilizes two types of inks: (I) Precursor ink prepared directly by dissolving metal salts in a solvent, [15, 60, 254] and (II) pre-synthesized CIGS NPs dispersed in a suitable solvents [187, 255]. In both approaches, selenization is performed after deposition to obtain large grained chalcopyrite phase. Selenization parameters such as temperature, time and selenium vapour pressure play an important role in achieving uniform, high-quality, phase pure large grained CIGSSe films [60, 256, 257]. It has been observed that substitution of sulfur by Se improves crystallization and eliminates void space [15, 187, 258, 259]. Grain growth during selenization efficiently reduces grain boundary concentration, potentially boosts carrier mobility and increases carrier collection thereby improving current generation [260–262].

Recently, Gonçalves *et al.* [227] reported wurtzite to chalcopyrite phase transformation at 478 ^{o}C for screen printed selenium based wurtzite $CuInGaSe_2$

NPs. This probably was the first report of demonstration of wurtzite to chalcopyrite phase transformation using in-situ powder XRD and TEM. However, no insight into the grain growth and phase transformation was offered. Carrete *et al.* [252] demonstrated wurtzite to chalcopyrite phase transformation and the consequent grain growth by selenizing a wz-CIGS film at 550 °C, however, mechanism of the phase transformation or grain growth was not discussed. Although the nucleation and growth mechanism during solution processing of metastable wz-CIS has been studied by several researchers [171, 172, 178, 184, 224], the phase transformation of wz-CIS to ch-CISSe and the grain growth during selenization has not been studied in sufficient detail.

VI.3 Experimental Procedure

Wurtzite-CIS Nanoparticle Ink Processing

The wz-CIS NPs (Average particle size ≈ 25 nm) were synthesized by a solution-based processing route **(Section III.2.3)**. The wz-CIS ink was prepared by dispersion of 260 mg of wz-CIS NPs in a mixture of toluene and 1-dodecanthiol (1-DDT) in a ratio of 10:2, and subsequently, it was kept under stirring for one day.

Spray Deposition of wz-CIS Films

The prepared wz-CIS ink was sonicated before deposition. The substrates were cleaned ultrasonically in acetone, isopropanol, and double-distilled water and was subsequently dried in an oven. The ink was deposited on commercially available soda-lime glass (SLG), and molybdenum-coated SLG (Techinstro, India) using spray deposition equipment (Holmarc Opto-mechatronics Pvt. Ltd., India) in an

open atmosphere while the substrate temperature was maintained at 250±5 °C. The schematic of the spray deposition system is shown in **Figure VI.1(a)**. The speed of the spray nozzle was set at 300 mm/s in the *x*-direction and 6 mm/s in the y-direction, while the precursor flow rate was 2 ml/min. The distance between the substrate (substrate size ≈ 25x80 mm) and the spray nozzle was ~10 cm. The solution flow rate was precisely controlled by a syringe pump, while compressed nitrogen gas was used to spray the wz-CIS NPs to avoid the formation of impure phases.

Selenization of wz-CIS Films

The deposited layers were selenized in a tubular furnace at temperatures varying from 350 to 550°C (Heating rate 20 °C/min) at an interval of 50 °C for 15 minutes holding. A schematic of the selenization setup is shown in **Figure VI.1(b)**. Selenium shots (weighing ≈ 48 mg each) were used as a source of Se. The films of size 25 mm x 20 mm and two selenium shots were placed inside a graphite box (~10 × 5 × 2 cm external volume), while the box was placed in the hot zone of the tubular furnace. Selenium shot to wz-CIS film distance is shown in **Figure VI.1(c)**. Selenization was carried out under the constant flow (flow rate of 20 sccm) of argon gas through a mass flow controller (Bronkhorst, Netherlands). The samples were allowed to cool naturally in the furnace after the selenization process. The selenized films, which were black in the beginning, turned grey, indicating the formation of ch-CISSe. The substrates were preheated at 120 °C in the tube furnace under vacuum for 10 minutes to remove any adsorbed moisture or oxygen from the substrates and quartz tube.

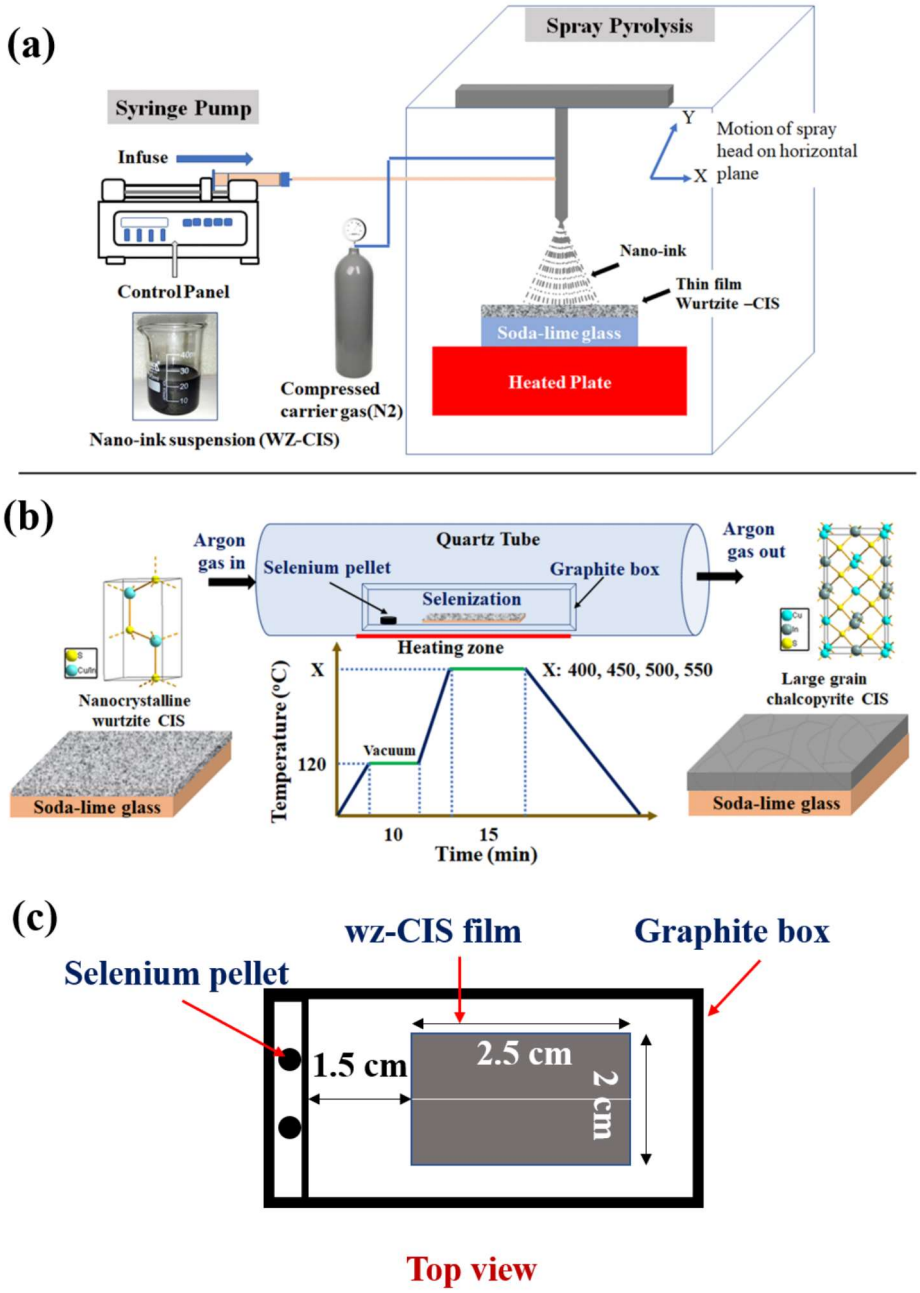

Figure VI.1 Schematic of (a) spray system for the deposition of wz-CIS thin film, (b) the selenization process for the preparation of a ch-CISSe absorber film, (c) Top view of graphite box showing the position of selenium and sample.

VI.4 Characterization

The crystallographic phase analysis of the deposited films was carried out by X-ray diffraction (XRD) (Rigaku Mini flex-600 (40 kV–15 mA); Rigaku, Tokyo, Japan) using CuKα radiation (λ=0.154 nm). XRD data were recorded in the 2θ scan range from 20-70°, at a step size 0.02° with a scan rate of 2°/min. The microstructural characterization was done using a field emission scanning electron microscope (FESEM: Nova Nano SEM 450, FEI Company of USA (S.E.A.) PTE, LTD). The energy dispersive X-ray spectra of the deposited film were acquired utilizing a customary unit (Pegasus Integrated EDS-EBSD with Octane Plus and Hikari Pro, EDAX Inc.) attached to the FESEM. For elemental analysis, K-emission lines for Cu and S while L-emission lines for In, Se, and Mo were utilized. The L-emission lines for In, Se and Mo were selected to fit all the emissions lines into one spectrum of 0 to 10 keV range to facilitate easy quantification. The K-level emission lines of In, Se, and Mo are in the range of 11-24 keV, which might introduce detector biasing error. The phase transformation and crystallization were investigated by using DSC-60 Plus (M/s Shimadzu (Asia Pacific) Pte Ltd.). The temperature scanning was done at a scan rate of 5, 10, 15, and 20 ℃/min in the temperature range of 40 ℃ to 550 ℃ under a nitrogen atmosphere for a powder mixture of selenium and wz-CIS.

VI.5 Results and Discussion

XRD pattern of the spray-deposited wz-CIS film **(Figure VI.2(a))** shows phase pure crystalline wz-CIS. In the XRD pattern, the diffraction peaks are located at 2θ values 26.32°, 27.76°, 29.82°, 38.64°, 46.50°, 50.38°, 54.22°, 54.98°, 56.22°,

57.38°, 61.92° and 64.20°, which could be assigned to the crystallographic planes $(10\bar{1}0)$, (0002), $(10\bar{1}1)$, $(10\bar{1}2)$, $(11\bar{2}0)$, $(10\bar{1}3)$, $(11\bar{2}2)$, $(20\bar{2}0)$, $(20\bar{2}1)$, (0004), $(20\bar{2}2)$ and $(10\bar{1}4)$ of the wz-CIS phase, respectively. No impurity peak could be observed, which indicates that even if some binary impurity phase was present, it was below the detection limit of the diffraction experiment. Our result is consistent with the pattern reported earlier by Pan *et al.* [44, 172] (a = b = 3.90 Å, c = 6.44 Å and space group: P63mc). A simulated X-ray pattern for wz-CIS is included for comparison at the lower panel of **Figure VI.2(a)**. The observed hump in the range of 2θ values 20 to 35º was due to the soda-lime glass substrate [263]. The high-resolution SEM cross-section image of wz-CIS/SLG shows uniform, dense wz-CIS NP film having an average grain size of 25±5.33 nm and film thickness of 2±0.1 μm, one such image is shown in **Figure VI.2(b)**.

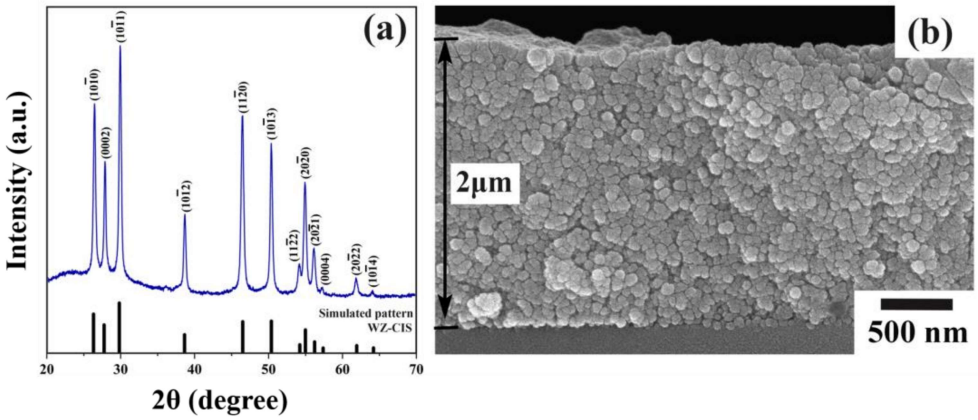

Figure VI.2 (a) X-ray diffraction pattern and (b) FE-SEM image of a cross-section view of the sprayed wz-CIS thin film on soda-lime glass.

The small grain size of absorber films is known to result in lower performance of thin-film solar cells devices, as it increases grain boundary volume fraction, which

acts as traps for charge carriers [40]. The elemental ratio Cu:In:S was around 1.0:0.78:1.7 (an average of more than five different points), which was very close to the expected 1:1:2 stoichiometry for $CuInS_2$ and falls within the CIS phase field in the wz-CIS phase diagram [89].

Selenization temperature and time play a crucial role in the microstructure evolution of the film and in turn, the device performance [264]. Selenization is known to result in the partial substitution of Se for S in wz-CIS to form ch-CISSe. The extent of Se substitution is governed by the selenium vapor pressure and the duration of selenization. The selenization of the films was carried out at varying temperatures in the range of 350-550℃ for 15 min. The grain growth and the change in Se/(S + Se) ratio were analysed after selenization. The XRD patterns of the ch-CISSe films, selenized at 350, 400, 450, 500, and 550℃ for 15 minutes, are shown in **Figure VI.3(a)**. The XRD pattern of the films selenized at 350 ℃ could be indexed to the wurtzite CISSe, indicating that the wurtzite phase was still intact. The XRD patterns obtained from the films selenized between 400-550 ℃ could be indexed to the ch-CISSe **(Figure VI.3(a))**, indicating the formation of ch-CISSe phase (space group $I\bar{4}2d$) [47, 143, 187, 252]. In addition, the doublet (204)/(220) and the triplet (116)/(312)/(215) peaks progressively became well defined and sharper, while the peak intensities increased with the selenization temperature, as shown in **Figure VI.3(b)**. The diffraction peaks becoming sharper and a gradual enhancement in peak intensities were attributed to the increased crystallinity and grain growth of the ch-CISSe phase with increasing selenization temperature.

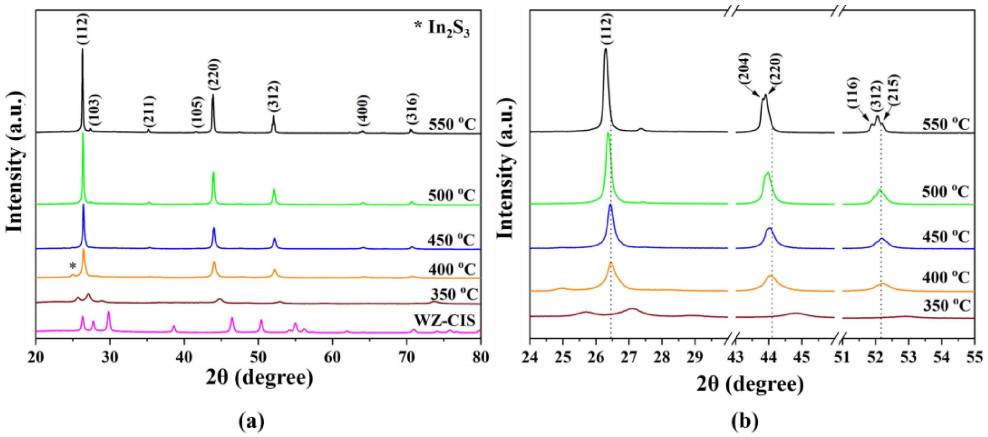

Figure VI.3 (a) XRD patterns of Ch-CISSe prepared by atmospheric selenization of sprayed wz-CIS layers at a variable temperature of 350, 400, 450, 500, and 550°C for 15 minutes, (b) Magnified view of the (112), (220), and (312) peaks showing a clear shift toward a lower angle.

At 350 °C selenization temperature, the wurtzite phase was still intact; however, no trace of the wurtzite phase **(Figure VI.3(a) (bottom))** was observed in the samples selenized at 400 °C. This shows that wz-CIS completely transformed to the chalcopyrite phase by 400 °C or the volume fraction of the wurtzite phase went below the detection limit by X-ray diffraction. This is contrary to the earlier report, where wurtzite to chalcopyrite transformation was observed to begin by 406 °C; however, the complete transformation took place by 600 °C [47]. An additional weak peak (at 2θ=25.02°) was observed in the case of the sample selenized at 400 °C, which matched with the (110) plane of In_2S_3 phase (ICSD:108563); however, just one peak cannot unambiguously confirm the presence of In_2S_3 phase. On selenization at higher temperatures i. e. 450, 500, and 550 °C, diffraction peaks shifted towards lower angles due to the greater selenium (Se) substitution where, the smaller sulfur (S) atoms (1.84 Å) were replaced by, the larger Se atoms (1.98

Å), as was reported earlier [187]. For instance, on selenization at 450 °C, the XRD peak corresponding to (112) of ch-CISSe reflection shifted to lower 2θ by Δ(2θ)=0.02º **(Figure VI.3(b))**, when compared to the samples selenized at 400 °C. On selenization at 500 °C, a greater shift of around Δ(2θ) = 0.1º in the (112) reflection toward a lower angle was observed when compared with its initial position at 400 °C. However, on selenization at the higher temperatures from 500 to 550 °C, the shift in diffraction peaks was marginal (Δ(2θ) = 0.04º). This could be due to the saturation of selenium substitution in the sample above 500 °C. The lattice parameters *a* and *c* were calculated from the 2θ values of all (*hkl*) planes using the equation [265]: $1/d^2=(h^2+K^2)/a^2+l^2/c^2$. As selenization temperature increased, both the lattice parameters *a* (from 5.81 to 5.84 Å) and *c* (from 11.63 to 11.69 Å) were observed to increase, while the *c/a* ratio did not change much, as shown in **Table VI.1**.

The cross-section FESEM images of the as-deposited wz-CIS film, the ch-CISSe film obtained after selenization at temperatures varying between 350-550°C (**Figure VI.4(a-f))**, and corresponding EDS results are shown in **Figure VI.4(g)**. The starting wz-CIS films had fine polygonal/equiaxed grains without much porosity **((Figure VI.4(a))**. On selenization at 350 °C marginal grain growth was observed without any significant change in morphology as shown in **(Figure VI.4(b)**. On raising the selenization temperature **((Figure VI.4(c-f))**, all the films transformed to ch-CISSe while the grain growth was dependent on the selenization temperature. This indicated that 400 °C is enough for the nearly complete wurtzite to chalcopyrite transformation. The images of the selenized ch-CISSe films **(Figure**

VI.4 (c-f)) show two distinct layers: a coarse/large-grained layer at the top and a fine-grained layer towards the substrate.

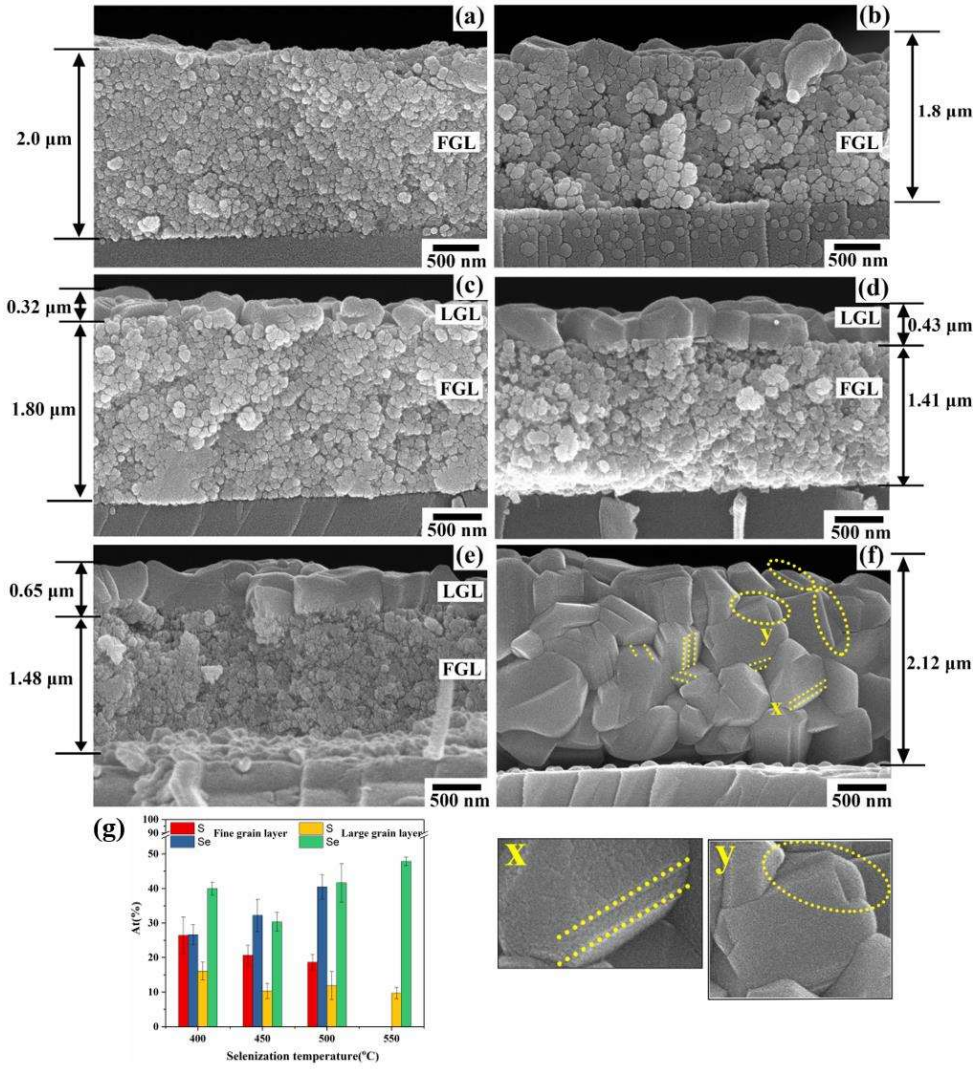

Figure VI.4 Cross-sectional FE-SEM images of (a) as-deposited wz-CIS film, ch-CISSe thin films obtained at varying selenization temperatures (b) 350, (c) 400, (d) 450, (e) 500 and (f) 550 °C. (g) atomic percent of sulfur and selenium in the fine-grained and the large-grained ch-CISSe layers. (Yellow dotted parallel line represents the twining defect (magnified image X) and ellipse represents the surface restructuring (magnified image Y)).

From the SEM images, it could be observed that the grain growth started from the top of the CIS layer and progressed towards the substrate with increasing temperature, indicating that the Se-vapour diffusion is probably the rate-controlling step for the grain growth. Greater selenization temperatures would increase the vapor pressure **(Figure VI.6(a))**. As a result, for the same processing time, greater Se could diffuse into the film, which causes a thicker large-grained layer. For instance, on selenizing at 400 °C for 15 min, films did not show any significant large-grained layer. The thickness of the large-grained layer increased progressively to cover almost the entire thickness of the film when selenization temperature was raised to 550 °C. An increase in temperature affects the diffusion of Se in two ways: (1) significantly raising the vapor pressure and (2) increasing the diffusion coefficient of Se into the film. Therefore, on increasing the temperature, the large-grained layer thickness progressed nonlinearly with increasing rate, as shown in **Figure VI.6(a)**. In the films selenized at 400 °C **(Figure VI.4(c))**, the coarse grained layer was only about 0.32 ± 0.05 μm thick, which increased to 0.43±0.07, 0.62 ± 0.04 and 2.12±0.12 on selenizing at 450, 500 and 550 °C, respectively for the same processing time (15 min). Chemical analysis **(Figure VI.4(g))** of the 400 °C selenized films revealed almost 50% Se for S in the fine-grained layer while the large-grained layer had about 71% Se substitution. Similarly, in all the cases, the large-grained layer had a significantly greater Se substitution compared to fined grain region **(Table VI.1)**. In the case of the sample selenized at 550 °C, the entire film was large-grained with a grain size close to 2.11 ± 0.12 μm **(Figure VI.4(f))**. This shows that even with a lower Se substitution, the phase transformation could happen; however, a greater degree of Se substitution is probably required for the grain growth. Earlier reports on Cu_2ZnSnS_4 (CZTS)

system, suggest that the wurtzite-CZTS to kesterite-CZTSSe phase transformation happens with significant grain growth during the selenization process [38, 41, 43]. Structurally both CZTS and CIGS are similar, with Zn and Sn being arranged in an orderly manner for kesterite-CZTS, whereas in ch-CIGS, In and Ga are randomly distributed.

Many literature reports [266–268] show the bilayer structure (large grain and fine/small grain layer). In general, the large-grained layer reduces the grain boundary volume fraction, which acts as trap for charge carriers [40], enhancing the absorption of long-wavelength photons [42]. The fine-grained layer, on the other hand, is generally believed to be detrimental to the device performance due to potential opportunity for recombination at grain boundaries and/or decreased carrier mobility [42, 269]. Interestingly, Wu *et al.* showed that the fine grains do not affect the device performance in their experiments [270]. Many of the earlier reports claimed that phase transformation and grain growth are related and happen together; however, from our study results **(Figure VI.3 and Figure VI.4)**, it can be concluded that, unlike CZTS, wurtzite to chalcopyrite transformation and grain growth are two independent phenomena in CIS. While, by 400 °C during heating in the presence of Se, wurtzite completely transformed to the chalcopyrite phase, the amount of Se diffusion and temperature was not sufficient for appreciable grain growth in 15 mins. In fact, wz-CIS film was selenized at 400 °C for 45 minutes and phase transformation from wz-CIS to ch-CISSe was observed, however, negligible change in the grain size happened. Chemical analysis showed about 50% Se for S substituted same as for 15 min selenization (**Figure VI.5**). As selenization temperature was raised to 450, 500, and 500 °C, the vapor pressure of Se (in turn

the driving force for diffusion) **(Figure VI.6(a))** and the diffusivity both increased and resulted in greater Se substitution for S, which facilitated the grain growth. This indicates that the grain growth is diffusion-controlled, while wurtzite to chalcopyrite phase transformation is not controlled by Se diffusion. Therefore, it can be concluded that by 400 °C, in the presence of Se vapor, the thermal activation was enough to trigger the wurtzite to chalcopyrite phase transformation, while a greater Se diffusion was required for the grain growth.

On careful observation, parallel linear contrast can be noticed in 550 °C selenized films (mark with yellow dotted parallel lines in **Figure VI.4(f)**). Recently, a similar feature in the CZTS was attributed to the formation of twins [271, 272]. Given the similarity in the structure, the linear contrast in this case probably arose due to the formation of similar twins in the ch-CISSe films. Substitution of larger Se atoms for the relatively smaller S atoms would strain the lattice and, as a result, increase the overall free energy, which would trigger defect formation (twining in this case) to accommodate the strain. The *c/a* ratio was more or less constant for samples selenized at varying temperatures **(Table VI.1)**. The observed twin formation may be attributed to the fact that whenever the volumetric strain builds up, such defects are introduced to relieve the lattice strain to reduce the overall free energy. Further, the large ch-CISSe grains were faceted, which indicated the surface restructuring process of grain (**Figure VI.4(f)**, a mark by a yellow color ellipse). Surface restructuring generally happens to bring the lower energy facets to the surfaces to facilitate overall energy minimization. This phenomenon has earlier been observed in alumina [273] and magnesia [274]. The formation of twins and surface

restructuring in ch-CISSe is interesting and warrants detailed high-resolution microscopy, which will be undertaken and communicated in the future.

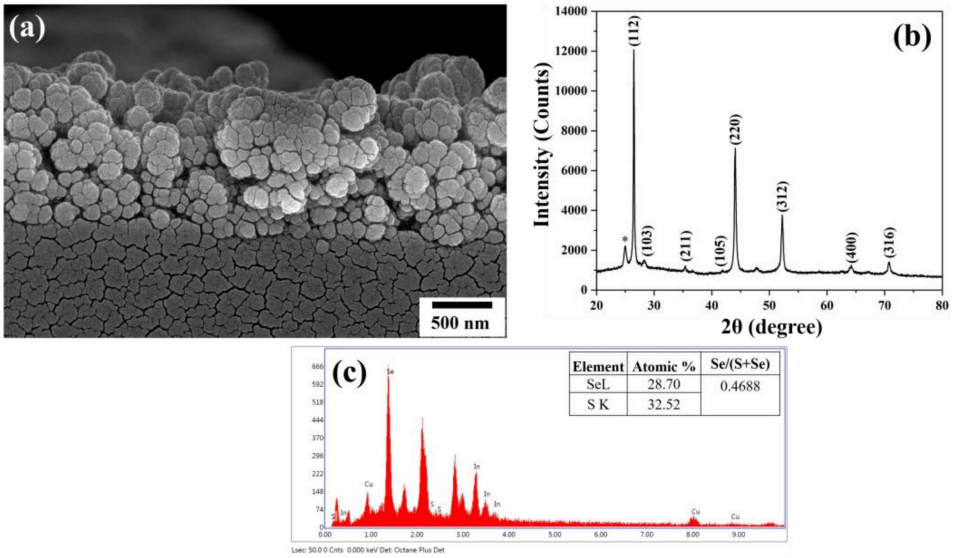

Figure VI.5 (a) FESEM image (b) XRD (c) EXD of selenized ch-CISSe at 400 ºC for 45 minutes.

Figure VI.6(b) and **(c)** showed the DSC curve of pure selenium and wz-CIS NPs, respectively. The DSC thermogram of the pure selenium showed two endothermic peaks, at 223 °C and 460-480 °C, corresponding to melting [275] and vaporization of the selenium powder, respectively. DSC thermogram of the pure wz-CIS had two endothermic peaks, at ~110 °C and ~200 °C, and a broad exothermic peak at around ~407 °C. The endothermic peaks at 110 °C and 200 °C were attributed to the dehydration of adsorbed water (indicated by X in **Figure VI.6(c)**, and the desorption of chemically adsorbed thiols molecules (indicated by Y in **Figure VI.6(c)**), respectively, while the exothermic peak at around ~407 °C (inset in **Figure VI.6(c)**) was attributed to the wurtzite to chalcopyrite phase transformation [47]. Inset in **Figure VI.6(c)** shows a discontinuity in the specific heat (ΔC_P), which

indicates to second-order character of the transition. **Figure VI.6(d)** depicts the DSC thermogram wz-CIS NPs added with Se powder at varying heating ramp rates of 5, 10, 15, and 20 °C/min.

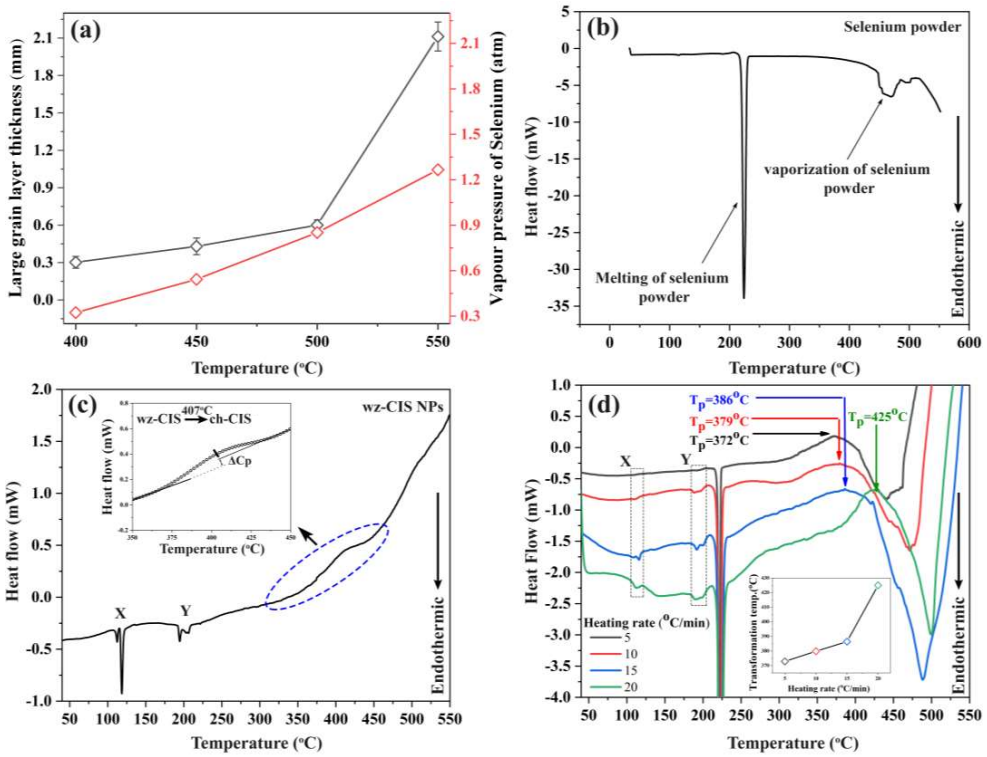

Figure VI.6 (a) Vapour pressure of selenium(calculated using equation [276]) and thickness of large grain layer versus selenization temperature. DSC curve (b) of Selenium powder and (c) pure wz-CIS NPs shows the phase transformation from wurtzite to chalcopyrite. The magnified view of the transformation range has been given in the inset. (d) DSC thermogram wz-CIS NPs added with Se powder at varying heating ramp rates of 5, 10, 15, and 20 °C/min with an inset of phase transformation temperature with respect to the varying heating rate. (X=Dehydration of water and Y= Desorption thiols molecules).

The three endothermic peaks were observed at ~114 ℃, ~207 ℃ and ~222℃, which could be attributed to the dehydration of adsorbed water (indicated by X in **Figure VI.6(d)**), the desorption of chemically adsorbed thiols molecules, which was used as sulfur source during synthesis of wz-CIS NPs (indicated by Y in **Figure VI.6(d)**) and melting of selenium powder, respectively. The exothermic hump at around 380-400℃ and the endothermic peak starting at around 500 ℃ could be attributed to the phase transformation of metastable wz-CIS to the stable ch-CISSe phase and the evaporation loss of Se/S, respectively. It was noticed that the exothermic peak, which was attributed to the wurtzite to chalcopyrite transformation shifted to higher temperatures with increasing heating ramp rates. The transformation temperatures were observed at 372, 379, 386 and 425 ℃ with increased heating ramp rates of 5, 10, 15, and 20 ℃/min, respectively (inset in **Figure VI.6(d)**). The increase in the transformation temperature with the increase in ramp rate may be attributed to the thermal inertia of the system. The increase in the transformation temperature with the ramp rate indicates that the wurtzite to chalcopyrite phase transformation has a strong second-order character. This observation is justified by the fact that the CIS is known to exist in three polymorphs: chalcopyrite, zinc blend and wurtzite **(Figure VI.7)** [89]. Chalcopyrite **(Figure VI.7(a))** and zinc blend **(Figure VI.7(b))** share a common …ABCABC… sulfur ion stacking planes ((112 and (111) in chalcopyrite and zinc blend, respectively). The cations (Cu and In), which occupies the tetrahedral interstitial sites, are ordered in chalcopyrite and disordered in zinc blend structure. On the other hand, in the wurtzite phase **(Figure VI.7(c))** the cations are disordered, while the sulfur ion stacking ((0002) plane) sequence is …ABAB... [47]. Therefore, for the wurtzite to transform into the chalcopyrite phase, not only the stacking sequence of

sulfur ions has to change, but the cations (Cu and In) have to be ordered. Therefore, the wurtzite-chalcopyrite transformation can have a second-order character. This further confirmed our assertion that phase transformation and grain growth are two distinct phenomena and are not coupled in the case of CIS.

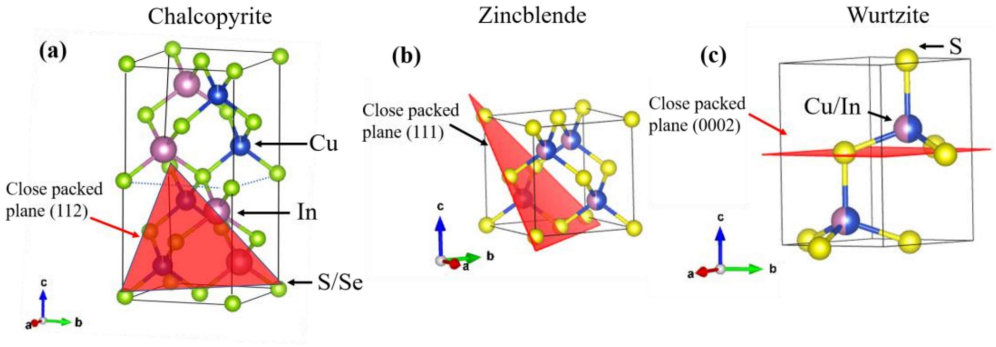

Figure VI.7 Crystal structures of (a) Chalcopyrite CISSe, (b) Zincblende CISSe and (c) Wurtzite CIS.

For actual application in solar cell devices, ch-CISSe is deposited on a Mo-coated SLG substrate. Therefore, to establish the applicability of the above findings, wz-CIS was deposited on the Mo-coated SLG and was selenized at 550 °C for 15 min to achieve a large-grained microstructure. The XRD spectra obtained from as-deposited wz-CIS/Mo/SLG film (bottom) show the wurtzite structure as seen in the case of deposition of wz-CIS on SLG **(Figure VI.8(a))**. All peak positions and planes are exactly similar to that deposited on SLG substrate, except for one additional peak at ~40º, which corresponds to Mo. On selenization, a phase change from wz-CIS to ch-CISSe occurred as observed from the XRD patterns **((Figure VI.8(a))**. Two additional peaks corresponding to the $MoSe_2$ phase were also observed in the selenized films. The formation of a thin layer of $MoSe_2$ is beneficial for the adhesion of the ch-CISSe layer [277]. The presence of a 100-200 nm thin

$MoSe_2$ interface layer reduces the Mo/ch-CISSe Schottky barrier height, thereby enhancing the FF and V_{OC}. On the other hand, a thicker layer of $MoSe_2$ increases the series resistance of the device, which can restrict the hole tunnelling [278, 279].

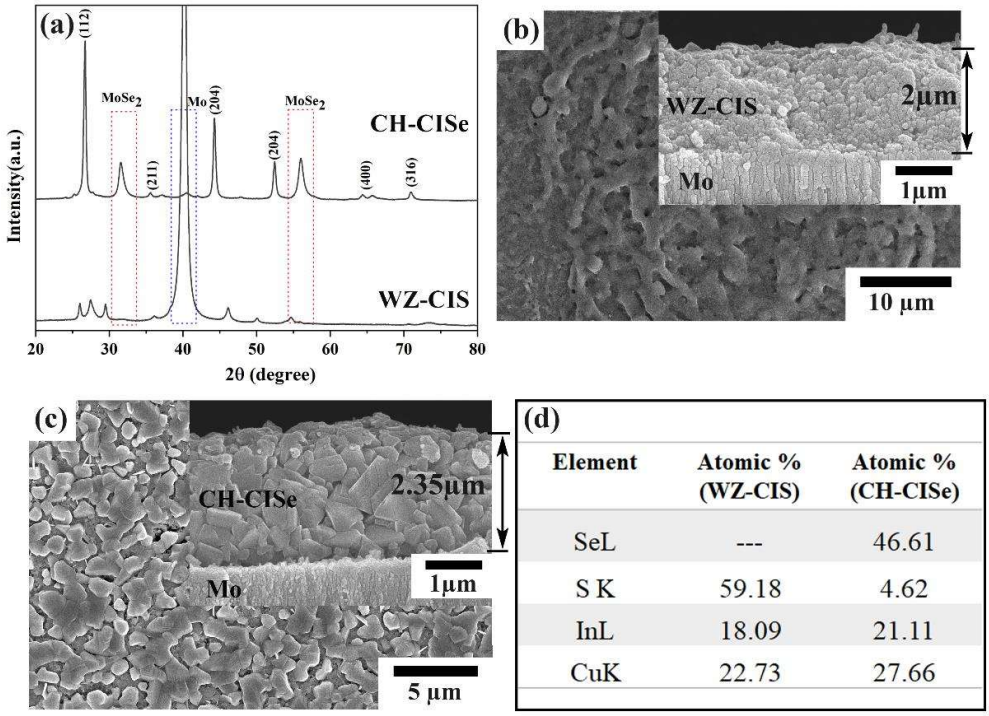

(d)

Element	Atomic % (WZ-CIS)	Atomic % (CH-CISe)
SeL	---	46.61
S K	59.18	4.62
InL	18.09	21.11
CuK	22.73	27.66

Figure VI.8 (a) XRD pattern of wz-CIS deposited on molybdenum coated SLG and selenized ch-CISSe film at 550 °C for 15 min (b) FESEM image of sprayed wz-CIS with cross-section view at the inset, deposited on molybdenum coated SLG (c) FE-SEM images of plane and cross-section view of ch-CISSe thin films obtained at 550 °C for 15 min (d) The elemental composition of the wz-CIS and ch-CISSe film.

The SEM image of spray deposited wz-CIS film, and the cross-section are shown in **(Figure VI.8(b))**. The deposited wz-CIS film is nearly uniform, having a dense structure without cracks or pinholes. The film thickness deposited by spray was 2.0±0.11 µm. The elemental composition using energy dispersive spectroscopy of

the wz-CIS layer showed **(Figure VI.8(d))** that the elemental ratio Cu:In:S was 1.0:0.80:2.60. On selenization, the complete wz-CIS layer transformed into ch-CISSe as shown in **Figure VI.8(c)**. The top plan view of ch-CISSe films revealed non-uniform grains; however, the cross-sectional view showed large-grained (grain size = 558±86 nm), compact microstructure having a thickness of around 2±0.22μm. EDS analysis reflected elemental composition ratio Cu:In: Se::1:0.78:1.7 **(Figure VI.8(d))**, which also very close to the ideal stoichiometric 1:1:2.

Table VI.1 Variation of lattice parameter and composition of fine-grain layer and large grain layer for selenization temperature.

Crystal Structure	**Selenization temperature (°C)**	**Lattice parameter (Å)**			**Composition variation**					
					Fine-grained layer (FGL)			Large-grained layer (LGL)		
		a=b	c	c/a	S (at%)	Se (at%)	Se/ (S+Se)	S (at%)	Se (at%)	Se/ (S+Se)
Wurtzite-CIS (Hexagonal)		3.921	6.424	1.638	---	---	---	---	---	---
	350	4.00	6.593	1.645	58	9	0.13	---	---	---
Chalcopyrite-CIS (Tetragonal)	400	5.804	11.627	2.003	26.45	26.62	0.50	16.07	39.97	0.71
	450	5.817	11.667	2.005	20.67	32.22	0.61	10.35	30.34	0.75
	500	5.821	11.671	2.004	18.65	40.49	0.68	11.86	41.66	0.78
	550	5.833	11.680	2.002	---	---	---	9.71	47.85	0.83

VI.6 Concluding Remarks

We studied the fabrication of chalcopyrite $CuIn(S,Se)_2$ (ch-CISSe) thin films on SLG and Mo-coated SLG substrate through a solution-based spray deposition route. The wz-CIS precursor was used as a precursor for achieving compact, large-grained ch-CISSe films. Selenization temperatures (400-550°C) are found to significantly

affect the morphology and grain size of the ch-CISSe films. The wurtzite-CIS films transformed completely to ch-CISSe by 400 °C. The surface morphology (FESEM) and elemental analysis (EDS) show the faceted grain growth throughout the thickness of the film with a maximum conversion ratio (Se/Se+S) at 550 °C on 15 min of selenization. The ch-CISSe film resulted in much larger grains of 700-750 nm as compared to spray deposited wz-CIS (25±5 nm). Our results showed that phase transformation and grain growth are not coupled in the case of CIS. The main conclusions of this study are:

1. The wurtzite to chalcopyrite transformation happened by 400 °C with much lower Se substitution (Se/(Se+S) ≈ 0.5), while the grain growth is temperature-dependent and requires greater Se diffusion (Se/(Se+S) > 0.7).
2. Wz-CIS to ch-CISSe transformation has a second-order character with a possible zincblende-CISSe intermediate phase.